EXPERIMENTAL AND NUMERICAL INVESTIGATIONS ON DUCTILE-TO-BRITTLE TRANSITION IN A CARBON STEEL

CHENG YAN, YIU-WING MAI and SHANG-XIAN WU

Center for Advanced Materials Technology, Mechanical & Mechatronic Engineering Department, The University of Sydney, NSW 2006, Australia

ABSTRACT

Using finite element analysis and metallographic observations, the stress field ahead of stationary and growing cracks and the ductile-to-brittle transition mechanism in a carbon steel have been evaluated. Compared to a stationary crack, a growing crack elevates both the stress triaxiality and the opening stress on the remaining ligament. The micro-criterion for cleavage fracture for both stationary and growing cracks is postulated to be identical. Ductile-to-brittle transition may occur as a result of increasing constraint for different specimen geometries. Based on the stress fields ahead of the stationary and growing cracks and the measured value of local cleavage stress, the ductile-to-brittle transition temperature has been successfully predicted in the compact tension (CT) specimen geometry.

KEYWORDS

cleavage fracture, transition, fracture toughness, constraint, finite elements.

INTRODUCTION

Many engineering structures of ferritic steel operate in the ductile-to-brittle transition region where unstable fracture occurs by transgranular cleavage after some amount of ductile crack growth. The prediction of the fracture transition is one of the remaining important problem to be addressed in fracture mechanics. To achieve this purpose, it is essential to understand the stress fields ahead of a growing crack and the fracture criterion for ductile-to-brittle transition. In the theoretical and numerical work by Rice and co-workers (1978, 1980), it was shown that the stress field ahead of a growing crack changed little from that of a stationary crack for elastic-ideally plastic solids under small scale yield condition. Also, the small strain finite element simulation of growing cracks by Xin and Goldthorpe (1993) indicated that the stress field ahead of a growing crack is basically the same as a stationary crack. However, in the work of O'Dowd, Shih and Dodds, Jr (1994), it was found that crack growth elevated the opening stress and shifted the location of peak stress closer to the crack tip. For cleavage fracture, a local failure criterion has been proposed (Ritchie *et al.*, 1973) such that cleavage occurs when the opening stress exceeds a critical cleavage stress over a characteristic distance ahead of the crack

tip. It is unclear, however, whether this criterion can be applied to cleavage fracture preceded by ductile crack growth. In the present work, the compact tension (CT) specimen was employed to measure the fracture toughness at different temperatures. Also, detailed microscopic observations were carried out to evaluate the variation of cleavage initiation position. Based on the CT test and the experimental work of Wu and Mai (1995) for three-point bend [SE(B)] and centre-cracked tension [M(T)] specimens, a large deformation finite element analysis was carried out to investigate the stress fields ahead of a growing crack for the different specimen geometries. The mechanism of ductile-to-brittle transition and the prediction of transition temperature are discussed.

EXPERIMENT AND FINITE ELEMENT ANALYSIS

The material used for the experiments was a carbon steel. The chemical composition of the steel is 0.25% carbon, 0.82% manganese, 0.21% silicon, 0.05% phosphorus and 0.03% sulfur. The stress-strain relationship is expressed by $\sigma=K\varepsilon^n$, where K is a constant and n is hardening exponent. The values of K, n and yield stress σ_o at different temperatures are given in Table 1.

Table. 1 Yield strength & hardening exponent of carbon steel

Temperature (°C)	Yield Strength (MPa)	Hardening Exponent	Constant K
30	226	0.23	662
20	236	0.23	715
0	250	0.25	904
-30	278	0.25	908
-50	296	0.25	943
-70	322	0.24	1066

The CT specimens (a/W=0.6) were tested from -70°C to 40°C. Crack tip opening displacement (CTOD) at unstable fracture (δ_c) was calculated according to ASTM standard E1290-93. Then δ_c was corrected for crack growth in terms of Hellmann and Schwalbe's equation (1986). The CTOD at ductile initiation, δ_i, was obtained by the resistance curve method. The SE(B) specimens (a/W=0.1) and M(T) specimens (a/W=0.5) were tested at 30°C by Wu and Mai (1995) and δ-Δa resistance curves were obtained. The thickness of all specimens was 25mm and the configuration of the specimens could be found in Wu and Mai (1995). All tests were carried out in an Instron 1195 testing machine with a crosshead speed of 1.0 mm/min. The test temperatures were controlled using a close-loop constant temperature chamber. The fracture surfaces of CT specimens fractured at -70°C and -30°C were observed using a scanning electron microscope (SEM). The distance (X_f) from cleavage initiation site to a blunting crack tip for the specimens with complete cleavage or a growing crack tip for the specimens with cleavage preceded by ductile growth were measured.

To obtain the stress distributions ahead of a growing crack for the above specimen geometries, large deformation plane strain finite element analysis was carried out with the finite element code ABAQUS (Hibbitt *et al.*, 1996). Four-node isoparametric elements with 2 by 2 Gauss quadrature were used. Only one half of the specimen was modelled because of symmetry. To simulate stable crack growth, small elements with equal width (0.1 mm) are placed in front of the crack tip, as shown in Fig. 1.

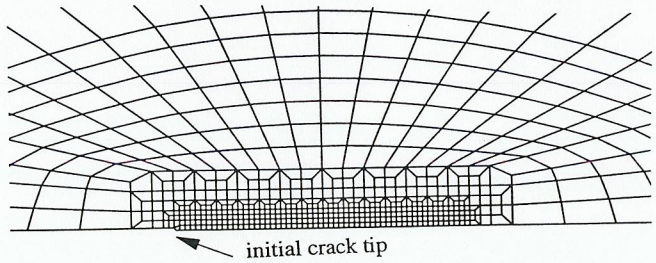

Fig. 1 Refined mesh for crack tip.

Rate-independent incremental plasticity and associated flow rule were used for the material constitutive model. Crack growth was achieved by the method of node release. Nodal forces of crack tip elements were reduced gradually to avoid numerical oscillation and non-convergence. When the calculated CTOD reached the measured initiation value, i.e., δ_i, the node at the crack tip was released. The crack growth was controlled by node release to ensure good agreement between the calculated CTOD and the experimental δ-Δa resistance curve.

STRESS DISTRIBUTIONS AHEAD OF A GROWING CRACK

The opening stress σ_{22}/σ_o distributions ahead of stationary and growing cracks for CT, M(T) and SE(B) specimens are shown in Fig. 2(a). It is clear that the opening stress increases after ductile crack growth. The position of peak stress shifts to the crack tip with crack growth when the distance is normalized as X/δ. This result is similar to the work of O'Dowd, Shih and Dodds (1994). The peak stress ahead of the crack tip increases in the order of M(T), SE(B) and CT specimens. The distribution of stress triaxiality ahead of the growing crack tip is shown in Fig. 2(b). Here stress triaxiality is expressed as the ratio of the hydrostatic stress σ_m over the Von Mises effective stress σ_e. The CT specimen has the highest stress triaxiality, i.e., highest constraint level and M(T) has the lowest. Fig. 3 shows the variation of peak opening stress with crack growth. It can be seen that the opening stress increases after the onset of ductile crack growth. After a certain amount of growth, σ_{22}/σ_o remains almost constant.

CONSTRAINT AND DUCTILE-TO-BRITTLE TRANSITION

The variation of toughness (δ_c) in CT specimens with temperature is shown in Fig. 4. At -70°C and -40°C, fracture occurred as complete cleavage for all specimens without any ductile crack growth. That is the specimens fractured at the lower-shelf region. At -30°C, -20°C, -10°C and 0°C, some CT specimens were cleavaged without ductile growth; but in some specimens cleavage was preceded by ductile crack growth. At 10°C, 20°C, and 30°C, cleavage was invariably preceded by ductile crack growth for all CT specimens. In contrast, at 30°C, SE(B) and M(T) specimens fractured in a complete ductile mode without displaying this transition behavior, showing the upper-shelf characteristic. Table 2 gives the measured distance X_f of cleavage initiation to the stationary crack (complete cleavage) or growing crack tips (cleavage preceded by ductile growth) at -70°C and -30°C for the CT specimens. The local cleavage stress σ_f is shown in Table 2.

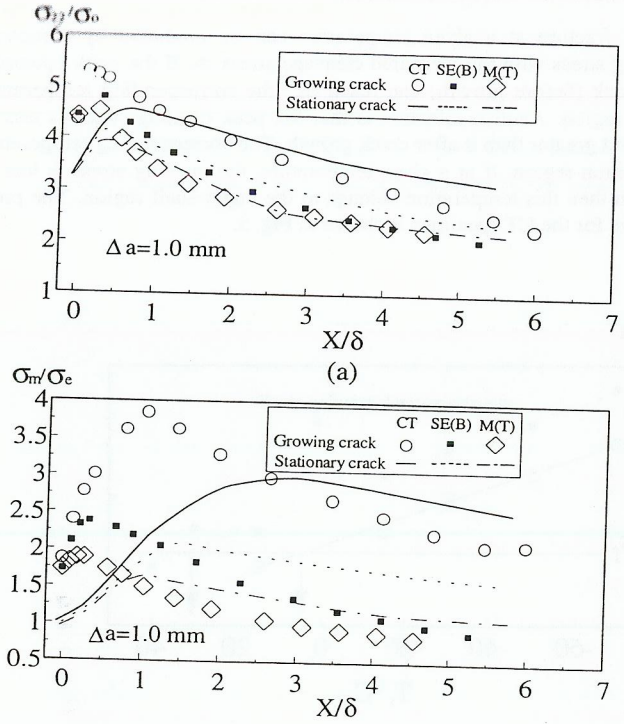

Fig. 2 Distributions of (a) opening stress σ_{22}/σ_o, and (b) stress triaxiality σ_m/σ_e.

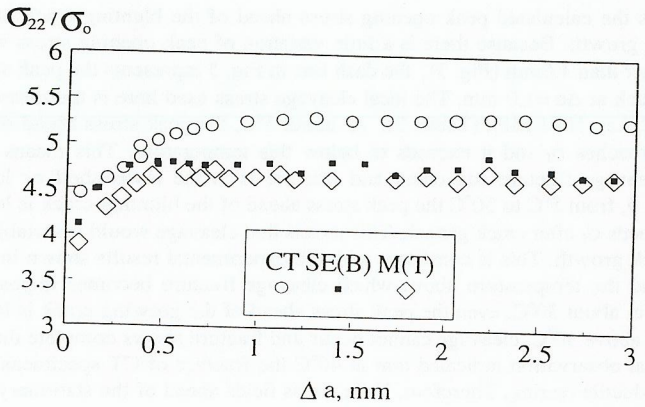

Fig. 3 Variation of peak opening stress (σ_{22}/σ_o) with loading.

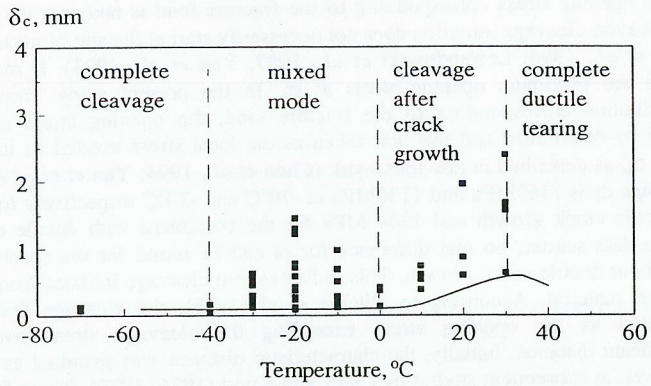

Fig. 4 Variation of toughness (δ_c) with temperature.

Table. 2 Experimental results of CT tests

T (°C)	X_f (μm)	X_f/δ_c	σ_f (MPa)	Δa (mm)
-70	209	2.55	1235	0
-70	300	2.34	1193	0
-70	350	4.41	1081	0
Average	286	3.10	1169	0
-30	382	1.67	1069	0
-30	188	1.54	1123	0
-30	428	1.41	1086	0
-30	436	1.71	1251	0
-30	367	1.26	1119	0
Average	360	1.52	1130	0
-30	1100	2.27	1116	0.34
-30	633	1.19	1212	0.53
-30	473	0.85	1299	0.66
-30	1000	1.59	1142	0.63
-30	400	0.88	1251	0.30
Average	721	1.35	1204	0.49

Usually, the maximum opening stress corresponding to the fracture load is taken as the local cleavage stress σ_f. However, cleavage initiation does not necessarily start at the site of maximum opening stress (Chen *et al.*, 1994; Lewandowski *et al.*, 1987; Yan *et al.*, 1993). It may be overestimated to take the maximum opening stress as σ_f. In the present study, from the calculated stress distribution corresponding to the fracture load, the opening stress at the initiation site X_f could be determined and this was taken as the local stress needed to initiate cleavage fracture, i.e., σ_f, as described in previous work (Chen *et al.*, 1994; Yan *et al.*, 1993) . From Table 2 the average σ_f is 1169MPa and 1130MPa at -70°C and -30°C respectively for the specimens without ductile crack growth and 1204 MPa for the specimens with ductile crack growth. In spite of the data scatter, no real difference for σ_f can be found for the specimens fractured with and without ductile crack growth. This indicates that cleavage initiates from the weakest particle of the material. According to Ritchie et al (1973), the cleavage fracture criterion was postulated as the opening stress exceeding the cleavage stress over a microstructurally significant distance. Initially, the characteristic distance was assumed as two grain diameters. However, in subsequent studies by Curry and Knott (1976, 1979), it was found that no simple relationship existed between grain size and characteristic distance and a statistical argument was introduced to explain the variation of characteristic distance. In Table 2, there is no fixed cleavage distance ahead of a crack tip. Table 3 shows the maximum opening stress the specimen has experienced during crack blunting (stationary crack) and ductile growth (up to Δa=3.0mm) at 30°C..

Table. 3 The maximum opening stress the specimens experienced

Specimens	σ_{max}, MPa (stationary crack)	σ_{max}, MPa (growing crack)
CT	994	1175
SE(B)	920	1062
M(T)	879	1037

Comparing Table 2 with Table 3, it is clear that the maximum opening stress ahead of the stationary crack tip for all specimens is less than the average σ_f. This indicates that complete cleavage fracture cannot occur for all specimens at 30°C. After ductile crack growth, for SE(B) and M(T) specimens, the peak opening stress approaches the lower bound of σ_f but is less than the average σ_f. On the other hand, for CT specimens the peak stress ahead of the growing crack is greater than the lower bound of σ_f and approaches the average σ_f. This is in agreement with the experimental results at 30°C at which the ductile-brittle transition occurred after some crack growth for CT specimens but no transition occurred for SE(B) and M(T) specimens. Therefore, specimen geometry has a remarkable effect on the ductile-to-brittle transition due to different constraint levels.

PREDICTION OF DUCTILE-TO-BRITTLE TRANSITION

Usually, to determine the ductile-to-brittle transition temperature, many tests must be done at different temperatures. As discussed above, the cleavage criterion for both stationary and growing cracks is identical, i.e., the opening stress exceeds the local cleavage stress σ_f over a characteristic distance which is related to the random distribution of brittle particles. The

possibility of cleavage fracture at a given temperature can be predicted by comparing the calculated peak opening stress with the measured cleavage stress σ_f. If the peak opening stress ahead of a blunting crack (before growth) can reach σ_f, the corresponding temperature falls within the lower-shelf region. Another situation is that the peak opening stress is less than σ_f during crack blunting but greater than it after crack growth. The corresponding temperature is in the ductile-brittle transition region. If at a given temperature, the opening stress is less than σ_f even after crack growth then this temperature belongs to the upper-shelf region. The prediction of transition temperature for the CT specimen is shown in Fig. 5.

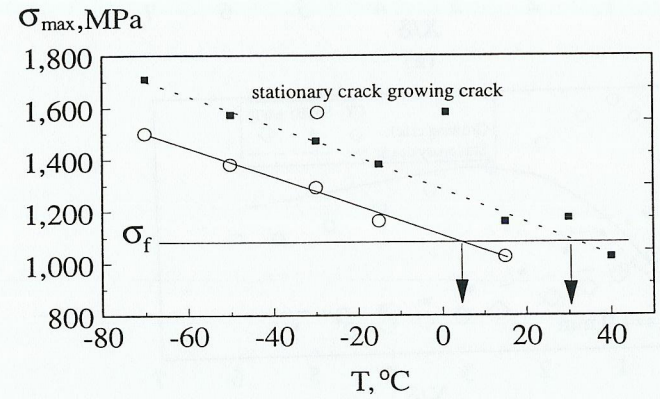

Fig. 5 Prediction of ductile-to-brittle transition behavior at different temperature

The solid line represents the calculated peak opening stress ahead of the blunting crack at the instant just before crack growth. Because there is a little variation of peak opening stress when crack growth Δa is greater than 1.0mm (Fig. 3), the dash line in Fig. 5 represents the peak stress ahead of the growing crack at Δa =1.0 mm. The local cleavage stress used here is the measured lower tail value at -70°C, i.e., 1081 MPa (Table. 2). At about 5°C, the peak stress ahead of the blunting crack just approaches σ_f and it exceeds σ_f below this temperature. This means that below 5°C complete cleavage fracture can occur and fracture is in the lower-shelf or lower transition region. In Fig. 5, from 5°C to 30°C the peak stress ahead of the blunting crack is lower than σ_f but its value exceeds σ_f after crack growth. This means that cleavage would invariably be preceded by ductile crack growth. This is consistent with the experimental results shown in Fig. 4. It is important to find the temperature above which cleavage fracture becomes impossible (upper-shelf). In Fig. 5, at about 30°C, even the peak stress ahead of the growing crack is lower than σ_f. This means that above 30°C, cleavage cannot occur and fracture shows complete ductile tearing. The experimental observation indicated that at 40°C the fracture of CT specimens was dominated by complete ductile tearing. Therefore, if the stress fields ahead of the stationary and growing cracks are known, the local cleavage stress σ_f can be obtained by locating the cleavage initiation position from the fracture surface. Then, the ductile-to-brittle transition temperature can be predicted by the method illustrated in Fig. 5.

CONCLUSIONS

Compared to a stationary crack, ductile crack growth elevates the stress triaxiality and opening stress on the remaining ligament and shifts the position of the peak opening stress to the growing crack tip. The cleavage criterion for both stationary and growing cracks is identical, i.e., the opening stress exceeds the local cleavage stress at a characteristic distance which is related to the random distribution of brittle particles. Specimen geometry has a remarkable effect on ductile-to-brittle transition due to the different constraint levels. Based on the stress fields ahead of stationary and growing cracks, the local cleavage stress can be obtained by locating the cleavage initiation position from fracture surface. A method for predicting the ductile-to-brittle transition temperature has been proposed and there is good agreement with the experimental data.

ACKNOWLEDGMENTS

The authors wish to thank the Australian Research Council (ARC) for the continuing funding of this project. C. Yan acknowledges the OPRS and UPRA awards by the University of Sydney. The Electron Microscope Unit of the University of Sydney has kindly provided access to its facilities.

REFERENCES

Chen, J.H., Yan, C. and Sun, J., (1994) *Acta metall.mater,* **42**, 251-261.
Curry, D.A. and Knott, J.F., (1976) *Metal Sci,* **10**, 1-6.
Curry, D.A. and Knott, J.F., (1979) *Metal Sci,* **13**, 341-345.
Hellmann, D.and Schwable, K.-H., (1986). In: *The Crack Tip Opening Displacement in Elastic-Plastic Fracture Mechanics* (K.H. Schwable, ed.), pp. 115-132, Springer-Verlag, Heideberg.
Hibbitt, Karlsson and Sorensen, (1996) *ABAQUS User's Manual*, Version 5.4., Providence, R.I.
Lewandowski, J.J. and Thompson, A.W., (1987) *Acta metall,* **35**, 1453-1462.
O'Dowd, N.P., Fong Shih, C. and Dodds, R.H., Jr, (1994). In: *Constraint Effect in Fracture: Theory and Application* (M. Kirk and A. Bakker, ed), ASTM STP 1244, pp. 134-159, Philadelphia.
Rice, J.R. and Sorensen, E.P., (1978) *J. Mech. Phys. Solids,* **26**, 163-186.
Rice, J.R., Drugan, W.J. and Sham, T-L., (1980). In *Fracture Mechanics: Twelfth Conference* (P.C. Paris, ed), ASTM STP 700, pp. 189-221, Philadelphia.
Ritchie, R.O., Knott, J.F. and Rice, J.R., (1973) *J. Mech. Phys. Solids,* **21,** 395-410.
Wu, S.X. and Mai, Y.W., (1995) In *Fracture Mechanics: 26th Volume* (W.G. Reuter, J.H. Underwood and J.C. Newman, ed), ASTM STP 1256, pp. 43-53, Philadelphia.
Xin, X.J. and Goldthoppe, M.R., (1993) *Fatigue Fract. Engng Mater. Struct,* **16**, 1309-1327.
Yan, C., Chen, J.H., Sun, J. and Wang, Z., (1993) *Metall. Trans,* **24A**, 1381-1389.